

Traveling wave antenna model of THz emission from a filament array

Sean D. McGuire^{1,*} and Mikhail N. Shneider²

¹Université Paris Saclay, Gif-sur-Yvette 91190, France

²Princeton University, Princeton, New Jersey 08544, USA

ABSTRACT. A simple traveling wave antenna model is used to theoretically study emission from an array of filaments. Both transverse and longitudinal arrays of filaments are considered. The angular distribution and power in the THz signal are significantly modified, which is consistent with other trends reported in the literature. The frequency content of the THz emission signal is also strongly modified under certain conditions. Whereas the emission from a single filament is broadband, the emission from a periodic transverse array consists of several discrete frequencies. For this latter case, the THz spectrum can be approximated as the product of two factors – the spectrum from a single filament and a complex frequency-dependent phase factor associated with the spatial distribution of the filaments. The complex phase factor accounts for interference effects, amplifying certain frequencies from the single filament spectrum while suppressing others. The location and width of the discrete frequencies present in the final spectrum depends on the number of filaments and their spacing. These results point to an interesting possibility of tailoring the frequency content in the THz signal.

I. INTRODUCTION.

Tailoring the frequency content of THz emission has been a topic of interest in the literature. One way to generate THz emission is by focusing femtosecond pulses onto nonlinear crystals, and several authors have looked at methods of controlling the frequency of this emission [1-5]. For example, D'Amico *et al* [1] and Vidal *et al* [2, 3] show that optical pulse shaping of the femtosecond laser can be used to produce narrowband tunable THz emission. Other work has shown that such pulse shaping can also be used to control the THz frequency via the 2-color mechanism in gas filaments [6, 7]. Fundamentally, these techniques rely on the interference between several THz pulses that are initiated in the active medium. Interference effects have been observed to occur in arrays of gas filaments as well, both when using the

1-color [8-13] and 2-color [14, 15] emission mechanisms. Such effects have been shown to significantly enhance the THz emission signal and alter the angular emission distribution relative to what is expected from a single filament. Furthermore, spectral alterations due to interference effects in a 2-filament array have also been experimentally demonstrated [16, 17].

We present a simple model capable of capturing interference effects in a filament array, which is based around the well-known Traveling Wave Antenna (TWA) model for the 1-color Transition-Cherenkov mechanism illustrated in FIG 1 [18, 19]. The calculations presented show that the spectrum of the THz signal from a filament array can be approximated as the product of two factors – the spectrum from a single filament and a complex frequency-dependent phase factor associated with the spatial distribution of

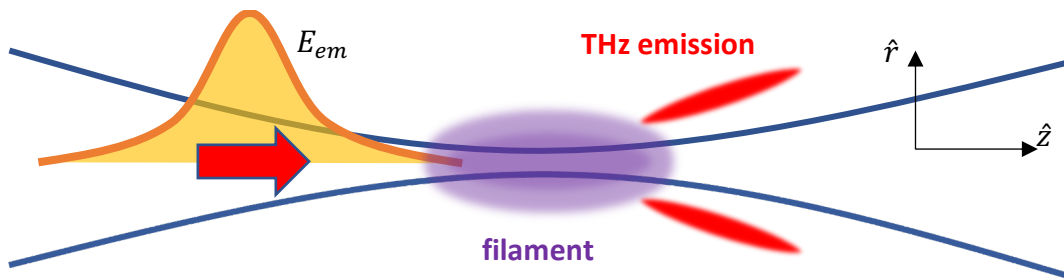


FIG 1: Experimental configuration used for the generation of THz radiation from a single filament. The direction of the emitted THz radiation depends upon the experimental parameters used but generally falls between the forward ($+z$) and side directions.

*Contact author: sean.mc-guire@centralesupelec.fr

the filaments. This complex phase factor accounts for interference effects and leads to significant alterations in the spectral content of the emission. Such alterations have been experimentally demonstrated for a 2-filament array [16, 17]. However, the calculations suggest that moving from a 2-filament to a multiple-filament array further accentuates this spectral modulation. For example, in the case of a transverse multiple-filament array considered below in Section IIIA, the spectral content consists of several narrowband emission peaks.

Recent work has shown that a slight modification of the underlying TWA model used here enables it to simulate emission due to the 2-color mechanism [20]. Therefore, though the 2-color is not considered in this paper, the conclusions drawn may also have implications for this method of THz generation.

II. MODEL

Following Zheltikov [18], the electric field emitted can be written as follows:

$$E(r, t) = \frac{\mu_0 c \sin \theta}{4\pi r \xi} \left\{ I \left[t - \frac{nr}{c} \right] - I \left[t - \frac{nr}{c} - \frac{L\xi}{u} \right] \right\} \quad 1$$

where θ is the angle between the axis of laser propagation and detector, r is the detector distance, I is the propagating current, $\xi = 1 - \beta n \cos \theta$, $\beta = u/c$, L is the length of the antenna, u is the speed at which the current propagates, and n is the index of refraction at the THz emission wavelength. A Fourier transform of this equation gives the following expression for the electric field:

$$\hat{E}_{SF}(\omega, \theta) = \frac{\mu_0 c}{4\pi r} \hat{i}(\omega) \frac{\sin \theta}{\xi} e^{-i\frac{\omega n}{c} r} \left[1 - e^{-i\frac{\omega L}{u} \xi} \right] \quad 2$$

$\hat{i}(\omega)$ is the Fourier transform of the laser-driven current $I(t)$, and is a complex variable. Taking the amplitude of $\hat{E}_{SF}(\omega, \theta)$ yields:

$$|\hat{E}_{SF}(\omega, \theta)| = \frac{\mu_0 c}{2\pi r} |\hat{i}(\omega)| \frac{\sin \theta}{\xi} \sin \left(\frac{\omega L \xi}{2u} \right) \quad 3$$

This is the expression provided by Zhao *et al* [19]. For the calculations below, $u = c$ and $n = 1$. Given these assumptions, Eqn. 3 becomes:

$$|\hat{E}_{SF}(\omega, \theta)| = \frac{\mu_0 c}{2\pi r} |\hat{i}(\omega)| \frac{\sin \theta}{1 - \cos \theta} \sin \left(\frac{\omega L}{2c} (1 - \cos \theta) \right) \quad 4$$

In this form, the TWA model is equivalent to the original analytic expression given by Amico *et al* [21] for the energy spectral density emitted per unit solid angle. The TWA model has been previously found to

yield reasonable agreement with experimental measurements of the angular distribution of emission – for example, see Buccheri and Zhang [22] or the results of Zhao *et al* [19].

The TWA model requires $\hat{i}(\omega)$ as an input. In a previous article [23], we developed a quasi-1D model for $\hat{i}(\omega)$ and compared the predictions from this model to a more detailed 3D axisymmetric numerical calculation based upon previous work published in the literature [24]. The simple 1D model, when used in conjunction with the TWA emission model, yielded predictions of THz emission power, frequency content, and angular distribution that were in good agreement with the more detailed numerical calculations. With this model, the current is calculated as follows:

$$\hat{i}(\omega) = \frac{\hat{\gamma}(\omega)}{i\omega + \nu_e} S \quad 5$$

with:

$$\gamma(\eta) = \gamma(\eta) \hat{z} = -\frac{1}{e\epsilon_0 c^2} \left(\frac{e^2}{m_e} \right)^2 \frac{1}{\omega_L^2 + \nu_e^2} * \left[\frac{n_0}{2} \frac{dI}{d\eta} + \nu_e n_0 I + I \frac{dn_0}{d\eta} \right] \quad 6$$

where $\eta = t - z/c$, $I(\eta) = (1/2)c\epsilon_0 \bar{E}_1 \bar{E}_1^*$ is the intensity of the laser, and $\hat{\gamma}(\omega)$ is the Fourier transform of $\gamma(\eta)$. ω_L is the carrier frequency of the laser.

Equations 4 – 6 require a certain number of inputs: the length of the antenna L , cross-sectional area of the antenna S , electron density n_0 , and laser pulse profile $I(\eta)$. These can all be estimated using a separate beam propagation model which predicts the evolution of laser intensity throughout the focal zone. Here, the beam propagation model described in Ref. [23] is used. In the results that follow, L is taken to be the FWHM of the axial density distribution on axis ($r = 0$). $A = \pi R^2$ where R is the FWHM of the radial density distribution, measured at the axial location of maximum density. n_0 is determined by using the multi-photon ionization rates of Mishima [25], which are a function of laser intensity.

The current profile $\hat{i}(\omega)$ is taken from calculations done in Ref. [23] and is shown in FIG 2, which also shows the THz emission from a single filament that results. This profile was calculated by simulating the focusing of a 50 fs and 800 nm wavelength pulse down using a 50 cm focal length lens. The pulse energy was 30 μ J pulse. The resulting filament length and radius were calculated to be $L = 2.5$ mm and $R = 7$ μ m. It is worth noting that, while the beam propagation model used here accounts for the nonlinear propagation effects of Kerr self-focusing

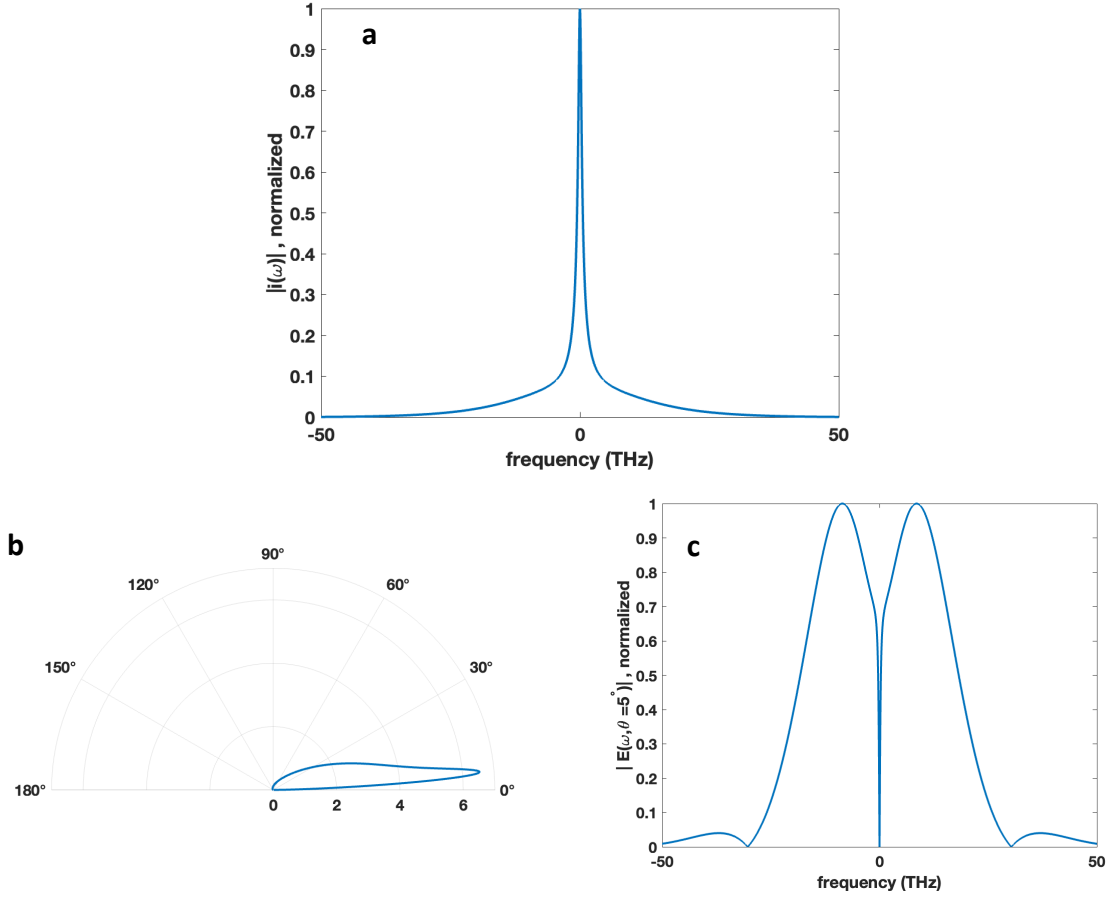


FIG 2: (a) Current profile $\hat{i}(\omega)$ used for the calculations shown in this paper. (b) Angular emission from a single filament with current profile $\hat{i}(\omega)$. Units of the radial axis are fJ/sr (i.e. energy per unit solid angle). (c) Frequency content of THz emission signal at the maximum emission angle of 5° .

and plasma defocusing, these effects are not expected to have a large impact of the frequency content and angular distribution of the emission [23]. Therefore, a much simpler linear gaussian propagation calculator could reasonably be expected to yield results that are very similar to what is presented here.

The emission from a generic distribution of several filaments can be calculated by summing the electric field from the individual filaments.

$$\hat{E}(\omega, \theta) = \sum_{m=0}^N (\hat{E}_{SF})_m \quad 7$$

In general, this is a vector sum given that the various $(\hat{E}_{SF})_m$ are vector quantities. The sum can be calculated numerically for an arbitrary distribution of filaments. We apply a few simplifying assumptions for all calculations. First, the filaments are assumed to be identical. Second, emission from one filament is assumed to be unimpacted by all other filaments. Third, the far-field approximation is invoked – the

spatial extent of the array is assumed much smaller than the distance to the detector (r). These assumptions significantly simplify Eqn. 7. Given that the filaments are identical and closely spaced relative to the detector distance, the vector electric fields $(\hat{E}_{SF})_m$ from the individual filaments can be assumed to share the same spatial orientation. Thus Eqn. 7 becomes a scalar sum. Additionally, the variables θ and r in Eqn. 2 are taken to be the same for various filaments: one important exception being within the exponential term $e^{-i\frac{\omega n}{c}r}$ where the variation in r cannot be ignored and accounts for interference between the emission from various filaments. This latter variation in r will be addressed below.

III. RESULTS

A. Transverse array of filaments

Although transverse bundles of femtosecond filaments have been shown to occur within a single focused

beam [26], the 1D periodic array discussed in this section would require the use of several beams. In this scenario, N filaments are organized into a 1D periodic array (spatial period D) orthogonal to the axes of laser propagation as shown in FIG 3. The filaments are assumed to be generated at the same moment in time. Note that the emission from a single filament is axisymmetric about the axis of laser propagation. However, the geometry proposed in FIG 3 results in THz emission that is not axisymmetric. The 1D filament array and detector define a plane, and the emission is altered upon rotation of this plane about any one of the filament axes. In the simple analytical expressions shown below, only the in-plane emission is considered. In this case, and setting $n = 1$, Eqn. 7 becomes:

$$\hat{E}(\omega, \theta) = \frac{\mu_0 c}{4\pi r_0} \hat{i}(\omega) \frac{\sin \theta}{\xi} * \left[1 - e^{-i\frac{\omega L}{u}\xi} \right] \sum_{m=0}^N e^{-i\frac{\omega}{c}r_m} \quad 8$$

Assuming that $ND \ll r_m$, r_m can be approximated as $r_m \sim r_0 + mD \sin \theta$ (where r_0 is the distance to the detector from the closest filament). Substituting into Eqn. 8 and simplifying gives:

$$\begin{aligned} \hat{E}(\omega, \theta) &= \frac{\mu_0 c}{4\pi r_0} \hat{i}(\omega) \frac{\sin \theta}{\xi} \left[1 - e^{-i\frac{\omega L}{u}\xi} \right] \\ &* e^{-i\frac{\omega}{c}r_0} \sum_{m=0}^N e^{-i\frac{\omega}{c}mD \sin \theta} \\ &= \left(\hat{E}_{SF} \right)_{r_0} \sum_{m=0}^N e^{-i\frac{\omega}{c}mD \sin \theta} \end{aligned} \quad 9$$

In other words, the electric field can be seen as the electric field from a single filament but modified by a phase factor which accounts for interference effects, and which mathematically corresponds to a Fourier series with a fundamental period of $c/D \sin \theta$ in frequency ($\Delta f = \Delta\omega/2\pi$) space.

FIG 4 and FIG 5 show the emission that results from a periodic array of $N = 2$ and $N = 10$ filaments. The

period between filaments was taken to be 1 mm . While the amplitude of the emission has significantly increased, this is to be expected as more filaments are radiating. The angular distribution of emission is not significantly impacted with respect to the emission from a single filament. However, the frequency content at the maximum angle of emission is significantly affected. Moving from a single filament to a periodic array results in a modulation of the frequency content. If more filaments are included, this effect becomes more pronounced such that the emission may be approximated as a sum of several discrete frequencies.

The observations above suggest that – given a particular $\hat{i}(\omega)$ – something approaching monochromatic emission can be obtained. Given the frequency bandwidth of the emission from a single filament (FIG 2c), the filament separation can be chosen accordingly. For the case considered, if the period is decreased to $D = 300 \mu\text{m}$, FIG 6 shows the resulting emission. The emission is now almost monochromatic – the central peak being at about 12 THz . Further increasing the number of filaments has makes the width of each resonant emission peak narrower and suppresses emission at other frequencies.

Eqn. 7 can also be used to model the emission from a more generalized transverse 2D mesh of filaments. We have performed such calculations and, aside from the lack of axisymmetry, the conclusions of the simple model below apply. Furthermore, by using a sufficiently large square array of filaments (e.g. 10×10), the emission can be rendered approximately axisymmetric upon rotation about an axis which is normal to the 2D plane of filaments, and which passes through the center point of the mesh. Using large numbers of filaments also results in a much larger THz emission signal. For example, a 10×10 periodic lattice (period $D = 1 \text{ mm}$) of filaments results in a maximum energy of 2.5 pJ/sr at

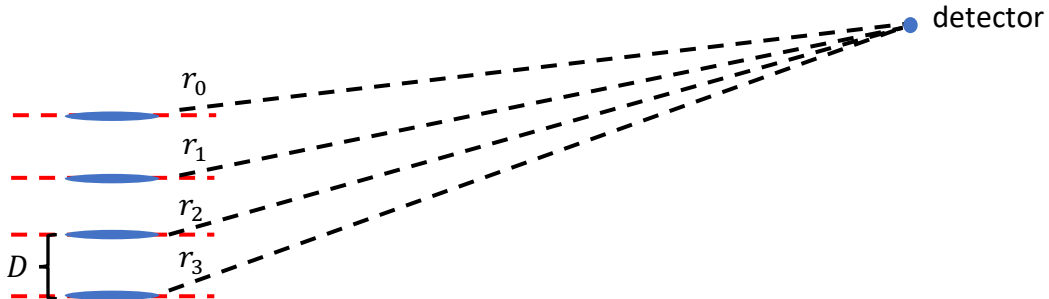


FIG 3: Periodic array of filaments, located distances of r_1, r_2, \dots , from the detector. The axes of laser propagation are indicated by the dashed red lines.

an angle of $\theta = 6.5^\circ$, versus $6 fJ/sr$ at an angle of $\theta = 5^\circ$ from a single filament (see FIG 2). This represents an increase of ~ 410 in the average intensity

of the THz signal, for a corresponding increase in laser energy of $10^2 = 100$.

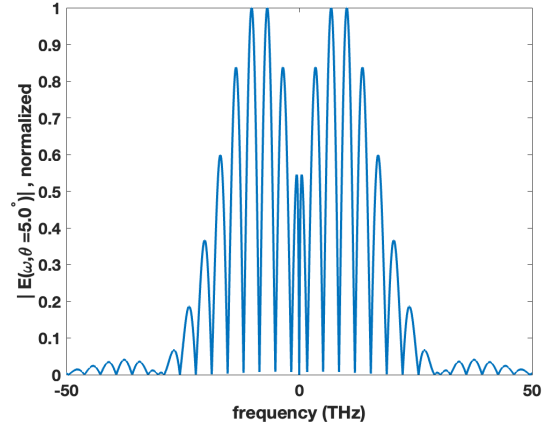
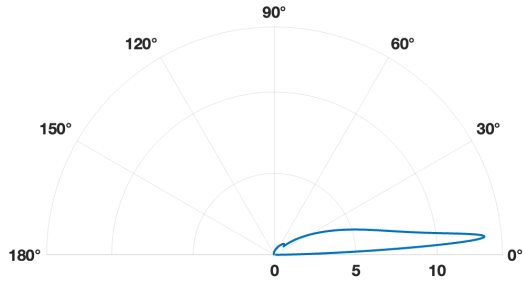


FIG 4: Angular distribution of emission in fJ/sr (left) and frequency content at the maximum angle of emission (right) for $N = 2$ and $D = 1 \text{ mm}$.

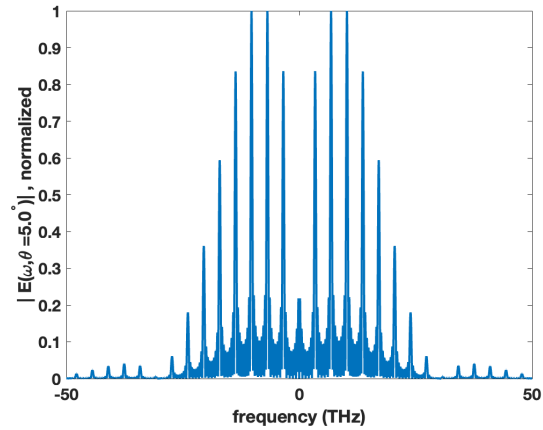
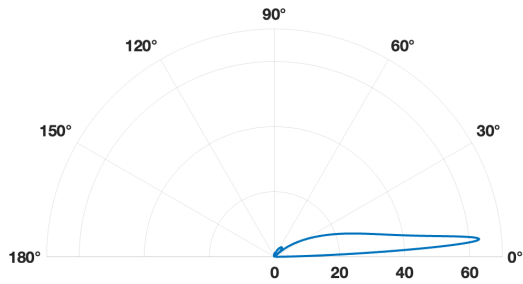


FIG 5: Angular distribution of emission in fJ/sr (left) and frequency content at the maximum angle of emission (right) for $N = 10$ and $D = 1 \text{ mm}$.

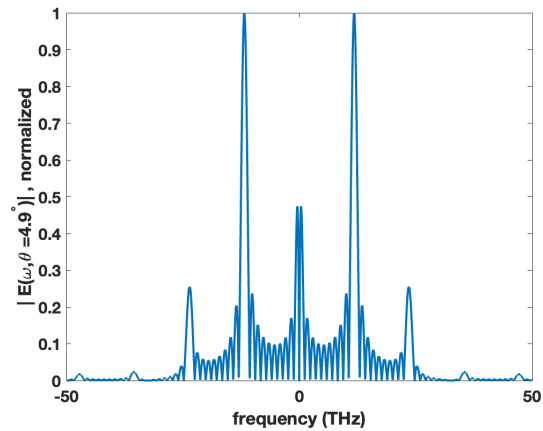
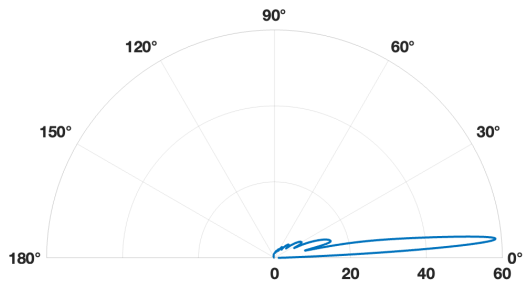


FIG 6: Angular distribution of emission in fJ/sr (left) and frequency content at the maximum angle of emission (right) for $N = 10$ and $D = 300 \mu\text{m}$.

B. Longitudinal array of filaments

The filaments in this scenario are spaced at periodic intervals along a single propagation axis – which could be the propagation of one or potentially several optical beams (FIG 7). This reconfiguration leads to three primary changes with respect to the case of a transverse array of filaments:

1. The distance to the detector becomes $r_m \sim r_0 + mD \cos \theta$ (where r_0 is the distance to the detector from the closest filament).
2. The filaments are not assumed to occur at the same moment in time. If these filaments are generated as a result of nonlinear propagation dynamics within a single beam, then each successive filament is initiated at a time delay of D/c , where c is the speed of light. The shift property of the Fourier transform implies that this leads to an additional phase factor for each successive filament, equal to $e^{i\omega mD/c}$. This phase factor should be applied to the current term associated with filament m .
3. The THz emission from the 1D array is axisymmetric about the array axis.

These changes lead to the following equation:

$$\begin{aligned} \hat{E}(\omega, \theta) &= \frac{\mu_0 c}{4\pi r_0} \hat{i}_0(\omega) \frac{\sin \theta}{\xi} \left[1 - e^{-i\frac{\omega L}{u} \xi} \right] \\ &* e^{-i\frac{\omega}{c} r_0} \sum_{m=0}^N e^{i\frac{\omega}{c} mD(1-\cos \theta)} \\ &= (\hat{E}_{SF})_{r_0} \sum_{m=0}^N e^{i\frac{\omega}{c} mD(1-\cos \theta)} \end{aligned} \quad 10$$

where $\hat{i}_0(\omega)$ should be understood to represent the current profile of the first filament (which is shifted in time from the current profile of the other filaments). Once again, $n = 1$ in the above relation.

FIG 8 and FIG 9 show the angular distribution and frequency content for a periodic filament spacing of $D = 1 \text{ mm}$ and for varying numbers of filaments. Here the frequency content at the maximum angle of emission is only slightly effected. Meanwhile, the angular distribution is affected in the sense that the emission becomes increasingly oriented towards the forward direction as N is increased.

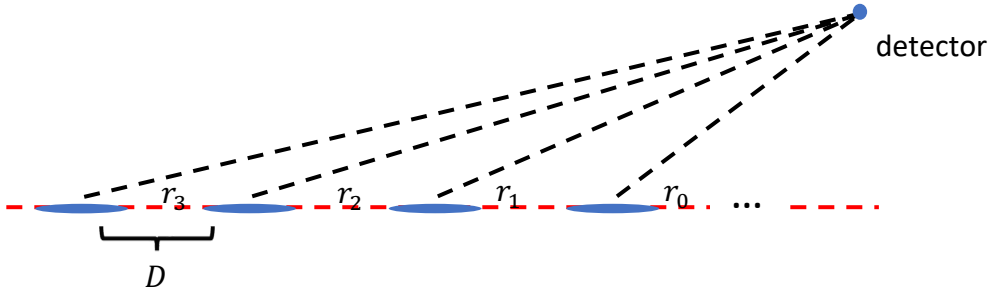


FIG 7: Periodic array of filaments, located distances of r_1, r_2, \dots , from the detector. The axis of laser propagation is indicated by the dashed red line.

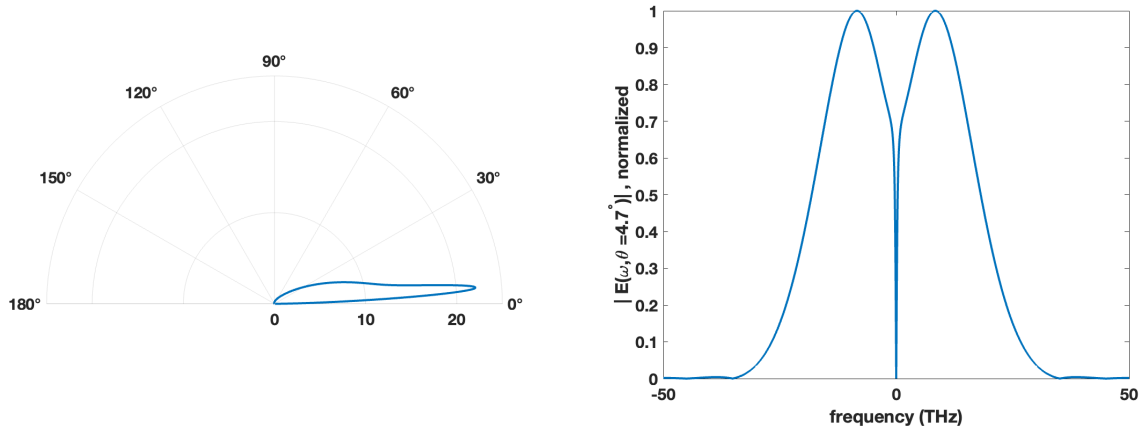


FIG 8: Angular distribution of emission in fJ/sr (left) and frequency content at the maximum angle of emission (right) for $N = 2$ and $D = 1 \text{ mm}$.

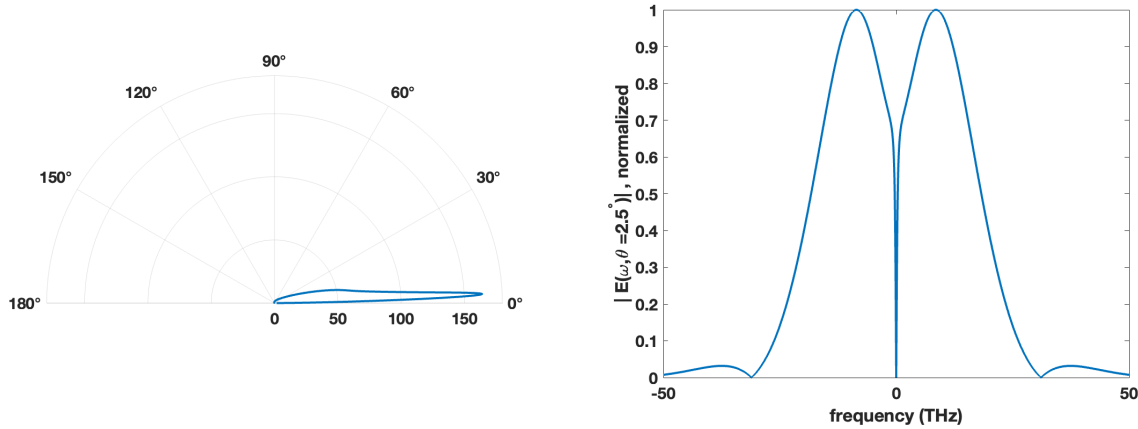


FIG 9: Angular distribution of emission in fJ/sr (left) and frequency content at the maximum angle of emission (right) for $N = 10$ and $D = 1$ mm.

V. CONCLUSIONS

THz emission from a periodic array of filaments is examined using a simplified TWA antenna formalism. The model developed here was used to study transverse and longitudinal periodic arrays. The input current profile $\hat{i}(\omega)$, filament length L , filament spacing D , and number of filaments N all play critical roles in the redistribution and frequency content of the emission. The transverse periodic array appears of particular interest as the frequency content in the signal can be significantly modified, leading to the emission of discrete frequencies and possibly quasi-monochromatic emission. Similar interference effects

have been experimentally observed for a 2-filament array [16], which suggests that the calculations shown here should remain valid for a multiple-filament array. Such an approach for tailoring the frequency content of the THz signal provides an alternative to existing approaches involving, for example, the use of nonlinear crystals [1-5] or metamaterials [27].

ACKNOWLEDGMENTS

This work was partially supported by the Princeton Collaborative Low Temperature Plasma Research Facility (PCRF).

1. D'Amico, C., et al., *Tuning and focusing THz pulses by shaping the pump laser beam profile in a nonlinear crystal*. Optics Express, 2009. **17**(2): p. 592-597.
2. Degert, J., et al., *Generation of Tunable THz Pulses*, in *Laser Pulses - Theory, Technology, and Applications*, I. Peshko, Editor. 2012.
3. Vidal, S., et al., *Femtosecond optical pulse shaping for tunable terahertz pulse generation*. Journal of the Optical Society of America B, 2010. **27**(5): p. 1044-1050.
4. Ovchinnikov, A.V., et al., *Generation of strong-field spectrally tunable terahertz pulses*. Optics Express, 2020. **28**(23): p. 33921-33936.
5. Shu, L., et al., *Quarter-cycle engineering of terahertz field waveforms*. Laser Physics Letters, 2014. **11**(8): p. 085404.
6. Lu, C., et al., *Controlling terahertz radiation in gas plasma with time-delayed laser pulses by the pulsing shaping technology*. Optik, 2019. **185**: p. 8-13.
7. Das, J. and M. Yamaguchi, *Tunable narrow band THz wave generation from laser induced gas plasma*. Optics Express, 2010. **18**(7): p. 7038-7046.
8. Tzortzakis, S., et al., *Coherent subterahertz radiation from femtosecond infrared filaments in air*. Optics Letters, 2002. **27**(21): p. 1944-1946.
9. Liu, Y., et al., *Terahertz Radiation Source in Air Based on Bifilamentation of Femtosecond Laser Pulses*. Physical Review Letters, 2007. **99**(13): p. 135002.
10. Xie, X., et al., *Enhancement of terahertz wave generation from laser induced plasma*. Applied Physics Letters, 2007. **90**(14): p. 141104.
11. Durand, M., et al., *Fine control of terahertz radiation from filamentation by molecular lensing in air*. Optics Letters, 2010. **35**(10): p. 1710-1712.
12. Mitryukovskiy, S.I., et al., *Coherent synthesis of terahertz radiation from*

- femtosecond laser filaments in air*. Applied Physics Letters, 2013. **102**(22): p. 221107.
13. Panov, N., et al., *Directionality of terahertz radiation emitted from an array of femtosecond filaments in gases*. Laser Physics Letters, 2014. **11**(12): p. 125401.
 14. Zhao, J., et al., *Simple method to enhance terahertz radiation from femtosecond laser filament array with a step phase plate*. Optics Letters, 2015. **40**(16): p. 3838-3841.
 15. Ushakov, A., et al. *Multiple Filamentation Effects on THz Radiation Pattern from Laser Plasma in Air*. Photonics, 2021. **8**, DOI: 10.3390/photonics8010004.
 16. Chen, Y., et al., *Spectral interference of terahertz pulses from two laser filaments in air*. Applied Physics Letters, 2015. **106**(22).
 17. Zhang, Y., et al., *Active modulation of the terahertz spectra radiated from two air plasmas*. Optics Letters, 2017. **42**(10): p. 1907-1910.
 18. Zheltikov, A.M., *Laser filaments as pulsed antennas*. Optics Letters, 2021. **46**(19): p. 4984-4987.
 19. Zhao, J., et al., *Traveling-wave antenna model for terahertz radiation from laser-plasma interactions*. SciPost Phys. Core 5, 2022. **46**.
 20. Zhu, F., et al., *Unified framework for terahertz radiation from a single- or two-color plasma filament*. Optics Letters, 2024. **49**(1): p. 41-44.
 21. Amico, C.D., et al., *Forward THz radiation emission by femtosecond filamentation in gases: theory and experiment*. New Journal of Physics, 2008. **10**(1): p. 013015.
 22. Buccheri, F. and X.-C. Zhang, *Terahertz emission from laser-induced microplasma in ambient air*. Optica, 2015. **2**(4): p. 366-369.
 23. McGuire, S. and M. Shneider, *Axisymmetric model for 1-color laser filament THz emission*. 2024: ArXiv (arXiv:2411.18963).
 24. Thiele, I., et al., *Theory of terahertz emission from femtosecond-laser-induced microplasmas*. Physical Review E, 2016. **94**(6): p. 063202.
 25. Mishima, K., et al., *Effect of quantum interference on tunneling photoionization rates of N₂ and O₂ molecules*. The Journal of Chemical Physics, 2005. **122**(10).
 26. Skupin, S., et al., *Filamentation of femtosecond light pulses in the air: Turbulent cells versus long-range clusters*. Physical Review E, 2004. **70**(4): p. 046602.
 27. Tan, L., D. Wang, and K.-D. Xu, *Terahertz metamaterials for spectrum modulation:*

structural design, materials and applications. Materials & Design, 2024. **244**: p. 113217.